Published in final edited form as:
Dev Cell. 2009 December ; 17(6): 811–822. doi:10.1016/j.devcel.2009.11.005.

Coordinated actions of actin and BAR proteins upstream of dynamin at endocytic clathrin-coated pits

Shawn M. Ferguson[1,4,5], **Andrea Raimondi**[1,4,5,*], **Summer Paradise**[1,4,5,*], **Hongying Shen**[1,4,5,*], **Kumi Mesaki**[1,4,5], **Agnes Ferguson**[3,5], **Olivier Destaing**[1,4,5], **Genevieve Ko**[1,4,5], **Junko Takasaki**[1,4,5], **Ottavio Cremona**[8], **Eileen O' Toole**[7], and **Pietro De Camilli**[1,2,4,5,6,†]

[1]Department of Cell Biology, Yale University School of Medicine, New Haven, CT

[2]Department of Neurobiology, Yale University School of Medicine, New Haven, CT

[3]Department of Neurology, Yale University School of Medicine, New Haven, CT

[4]Howard Hughes Medical Institute, Yale University School of Medicine, New Haven, CT

[5]Program in Cellular Neuroscience, Neurodegeneration and Repair, Yale University School of Medicine, New Haven, CT

[6]Kavli Institute for Neuroscience, Yale University School of Medicine, New Haven, CT

[7]Boulder Laboratory for 3D Electron Microscopy of Cells, Department of Molecular, Cellular and Developmental Biology, University of Colorado, Boulder, CO

[8]IFOM, the FIRC Institute for Molecular Oncology Foundation, and Università Vita – Salute San Raffaele, Milano, Italy

SUMMARY

The GTPase dynamin, a key player in endocytic membrane fission, interacts with numerous proteins that regulate actin dynamics and generate/sense membrane curvature. To determine the functional relationship between these proteins and dynamin, we have analyzed endocytic intermediates that accumulate in cells that lack dynamin (derived from dynamin 1 and 2 double conditional knockout mice). In these cells, actin nucleating proteins, actin and BAR domain proteins accumulate at the base of arrested endocytic clathrin-coated pits where they support the growth of dynamic long tubular necks. These results, which we show reflect the sequence of events in wildtype cells, demonstrate a concerted action of these proteins prior to, and independent of, dynamin, and emphasize similarities between clathrin-mediated endocytosis in yeast and higher eukaryotes. Our data also demonstrate that the relationship between dynamin and actin is intimately connected to dynamin's endocytic role and that dynamin terminates a powerful actin- and BAR protein-dependent tubulating activity.

†To whom correspondence should be addressed. pietro.decamilli@yale.edu.
*These 3 authors contributed equally.

INTRODUCTION

Endocytosis is the fundamental process in cell physiology through which portions of the plasma membrane, along with extracellular material, are internalized. Among the many forms of endocytosis that operate in cells of higher eukaryotes, clathrin-mediated endocytosis is the most extensively characterized (Kirchhausen, 2000; Conner and Schmid, 2003; Robinson, 2004; Doherty and McMahon, 2009; Traub, 2009). This process starts with the assembly at the plasma membrane of coat proteins, progresses via the growth and invagination of the coated bud and is terminated by its fission in a reaction that involves the GTPase dynamin (Takei et al., 1995; Hinshaw, 2000; Pucadyil and Schmid, 2009). Each of these steps and their coordination requires a variety of accessory factors, most of which are conserved from yeast to mammals. Yet, in spite of the many similarities that have recently emerged between clathrin-mediated endocytosis in yeast and metazoan cells, important questions on the precise relationship between these two processes remain open.

In yeast, endocytosis involving clathrin occurs at so-called actin patches and is critically dependent on actin (Kaksonen et al., 2005; Kaksonen et al., 2006; Idrissi et al., 2008). Assembly of the coat is followed by the recruitment of actin nucleating proteins that initiate an inward movement of the coated membrane patch. This movement correlates with the formation of a tubular invagination surrounded by BAR proteins that eventually undergoes fission by an as of yet unclear mechanism. Most strikingly, there is lack of evidence for the role of an endocytic dynamin in this organism. While a protein, Vps1, that shares homology to dynamin is present in yeast, this protein does not appear to have a role in endocytosis (Kaksonen et al., 2006).

Conversely, in cells of higher eukaryotes, dynamin plays a major role in the fission reaction and an obligatory contribution of actin has been questioned. Actin nucleating proteins can be detected on at least a subset of clathrin coated pits, and actin disrupting drugs, such as latrunculin, were shown by some studies to inhibit clathrin-mediated endocytosis (Merrifield et al., 2005; Moskowitz et al., 2005; Yarar et al., 2005). Yet, the occurrence of latrunculin-insensitive, clathrin-dependent, endocytic reactions have also been reported (Moskowitz et al., 2005; Yarar et al., 2005; Saffarian et al., 2009). Thus the importance and mechanism of action of actin in clathrin-mediated endocytosis remain unresolved.

Interestingly, dynamin binds a large variety of actin regulatory proteins either directly or indirectly (Orth and McNiven, 2003; Schafer, 2004; Itoh and De Camilli, 2006), supporting a link between clathrin-mediated endocytosis and actin in metazoan cells. However, dynamin closely co-localizes with the protein network that controls N-WASP/Arp2/3 mediated actin nucleation even in cellular contexts that do not appear to be directly implicated in endocytic fission, such as membrane ruffles (Orth and McNiven, 2003), podosomes (Ochoa et al., 2000) and actin tails (Lee and De Camilli, 2002; Orth et al., 2002).

We speculated that studies of cells lacking dynamin expression might help to provide new insight into these questions. Studies of cells expressing dominant-negative dynamin mutants or treated with drugs that block dynamin have been very useful to explore dynamin function (Herskovits et al, 1993, van der Bliek et al, 1993 and Macia et al, 2006). However, mutant dynamin or pharmacologically blocked dynamin may act at least in part indirectly by sequestering other factors. Thus, results of these studies may not yield precisely the effect of lack of dynamin. Mammalian genomes comprise three dynamin genes: dynamin 1 (gene symbol Dnm1), which is expressed primarily in the nervous system (Ferguson et al., 2007), dynamin 2 (Dnm2) which is ubiquitously expressed (Praefcke and McMahon, 2004; Ferguson et al., 2007) and dynamin 3 (Dnm3), which is expressed primarily in brain and testis (Cook et al., 1996; Ferguson et al., 2007). So far, studies of cells that lack dynamin expression altogether have not been reported. Studies of dynamin 2 KO fibroblast-like cells showed a partial

impairment of clathrin-mediated endocytosis as well as of several other cellular functions, but interpretation of the results was complicated by the expression of dynamin 1 in these cells (Liu et al., 2008).

Towards the goal of gaining insight into dynamin's action relative to other endocytic factors and to actin, we used a conditional gene KO approach in mice to generate cells that lack dynamin. In these cells, a powerful and global impairment of clathrin-mediated endocytosis was accompanied by a dynamic actin-dependent tubulation of the neck of arrested coated pits and by an accumulation of N-WASP/Arp2/3, other actin nucleation factors and BAR proteins at these invaginations. Proteins present at such sites and their sequence of recruitment demonstrate a strong similarity of these structures to yeast actin patches. These results provide important new evidence for a major conservation of critical aspects of clathrin mediated endocytosis from yeast to man. They additionally contribute genetic data to support the hypothesis that BAR domain coated tubular necks represent actin-dependent templates on which dynamin assembles to promote fission.

RESULTS

Disruption of the Dynamin 2 Gene

Dynamin 2 is ubiquitously expressed and represents the major and perhaps only dynamin isoform expressed in most non-neuronal cells in an intact organism. Dynamin 2 has never been knocked-out at the whole organism level. Toward the goal of generating cells that lack dynamin, we first targeted the Dnm2 gene (Fig. S1). The KO of dynamin 2 resulted in early embryonic lethality [genotyping of 9 litters (between embryonic days 8 and 12) from heterozygote matings identified 19 wildtype (WT), 45 heterozygote and 0 KO embryos, $p=1.8\times10^{-5}$, χ^2 test], while homozygous conditional KO (dynamin $2^{LoxP/LoxP}$) mice were healthy and fertile as expected. Dynamin 2 KO cells were obtained from primary cultures of fibroblasts of these conditional KO mice following expression of Cre recombinase. Pilot experiments revealed defects in clathrin-mediated endocytosis in these cells (Fig S2A). However, as also reported recently (Liu et al., 2008), we found that cultured fibroblasts expressed dynamin 1 (Fig. S2B), although not detectable levels of dynamin 3 (Fig. 1A and S2C); and that over time in culture dynamin 1 levels increased (Fig S2B) with a corresponding recovery of endocytic function.

Generation of Conditional Dynamin 1/Dynamin 2 DKO Cells

Dynamin $2^{LoxP/LoxP}$ mice were interbred with newly generated conditional (see methods, Fig. S1) or germline dynamin 1 KO mice (Ferguson et al., 2007) and with mice expressing 4-hydroxy-tamoxifen (OHT) inducible Cre recombinase (Cre-ER), to obtain animals with the following two genotypes: $Dnm1^{-/-}$;$Dnm2^{LoxP/LoxP}$ and $Dnm1^{LoxP/LoxP}$;$Dnm2^{LoxP/LoxP}$;CRE-$ER^{+/0}$. Dynamin 1, dynamin 2 double KO (DKO) cells were subsequently derived from fibroblasts of these mice either by viral delivery of Cre recombinase or by exposure to 4-hydroxy-tamoxifen respectively. In both cases, Cre recombinase activity resulted in depletion of total dynamin content, as shown by immunoblotting with antibodies specific for dynamin 1, 2 and 3 respectively and with pan-dynamin antibodies (Fig. 1A and B and S2B). By immunofluorescent staining for dynamin we observed that there was a residual population comprising less than 5% of the cells in which Cre was ineffective/not expressed. DKO cells obtained by the tamoxifen inducible KO method were used for a further in depth study.

DKO Cells are Viable but have Endocytic Defects

Although a major defect in proliferation was present in DKO cells (Fig.1C and D), surprisingly these cells remained viable for at least 4 weeks in culture and their overall appearance was

grossly normal. In these cells, clathrin coat components were present at wild type levels (Fig. 1A and B). However, clathrin-mediated endocytosis was drastically impaired, as demonstrated by i) lack of transferrin uptake (Fig. 1E and F), ii) a corresponding accumulation of endogenous and transfected transferrin receptor at the cell surface as revealed both by immunofluorescence and by accessibility to cell surface biotinylation (Figure 1G, H and I, Fig. S2B), iii) an increase in the number of endocytic clathrin-coated pits with a clustering in their distribution (Fig 1J,K and L, S3A and B) and iv) an increase in their stability as demonstrated by time-lapse imaging of GFP-tagged μ2-adaptin (a subunit of the endocytic clathrin adaptor AP-2 complex, Fig. 1 M). Hence, we conclude that endocytic clathrin-coated pits still formed, but maturation to free clathrin-coated vesicles was dramatically impaired in the absence of dynamin. The accumulation of clathrin-coated pits in DKO cells could be rescued by electroporation of dynamin 2-GFP cDNA but not by a dynamin 2-GFP mutant that lacked the C-terminal proline rich domain (dynamin 2ΔPRD-GFP, Fig. 1L). Notably, no parallel alterations in the pattern of immunofluorescence (overall distribution and intensity) for clathrin and for the clathrin adaptor γ-adaptin were observed in the Golgi complex (Fig. S2C and D). The changes in the staining pattern for endocytic clathrin-coated pits in DKO cells were also observed (albeit in a more limited way) in cells where the expression of dynamin 1 and 2 was suppressed with siRNA (Fig. S1 F and G).

At least some other forms of endocytosis occurred in the absence of dynamin. For example, uptake of the membrane dye FM1-43 was not decreased, but rather slightly increased relative to controls (Fig. 1N and O). Furthermore, addition of growth factors still stimulated membrane ruffling and the formation of Rab5-positive macropinosomes in the absence of dynamin (Movie S1).

Dynamin has been implicated in the fission of caveolae from the cell surface (Henley et al., 1998). The loss of dynamin expression has complex effects on this process as revealed by an overall decrease in caveolin 1 levels (Fig. 1B), an altered localization of the remaining caveolin 1 as assessed by immunofluoresence (Fig. S2E) and a major reduction (>4 fold) in the overall number of caveolae at the plasma membrane as revealed by electron microscopy (Fig. S2F). These changes with respect to caveolae do not parallel the phenotype observed for endocytic clathrin-coated pits (i.e. an increased abundance due to impaired fission). They may reflect an indirect effect and were not investigated further. Likewise, while, as recently reported in dynamin 2 knockdown cells (Tanabe and Takei, 2009), there was a pronounced increase in the levels of acetylated-tubulin in DKO cells (Fig. 1B), the relationship of this phenotype to the direct actions of dynamin was not explored further.

Tubulation of the Plasma Membrane in DKO Cells

To precisely determine at which stage clathrin-mediated endocytosis becomes dynamin-dependent, electron microscopy was performed. The most unique and striking feature of DKO cells was the abundance of clathrin-coated pits connected to the plasma membrane by long, narrow, meandering tubules (Fig. 2), with an average diameter of 36+/−1nm (n=69 tubules, Fig. S3A) although shallow and constricted/omega shaped clathrin-coated pits budding from the outer cell profile were also visible (Fig. 2A, B and H). The 3-dimensional structure of the tubules and their relation to clathrin-coated pits in DKO cells was further investigated by electron tomography. This method showed that most tubules were clearly capped with a coated bud and that all clathrin-coated vesicular structures located in the cortical cytoplasm were connected to the surface by the tubules (>500nm long in some cases, Fig. 2J).

The accumulation of endocytic tubulated clathrin-coated pits occurred both on the ventral and on the dorsal portion of cells (Fig. 2I). No accumulation of clathrin-coated pits was observed in the trans-Golgi network area in agreement with immunofluorescence observations (see Fig. S2C and D). We conclude that dynamin, a membrane tubulating protein itself in vitro (Sweitzer

and Hinshaw, 1998;Takei et al., 1998;Takei et al., 1999), acts to terminate a membrane tubulating action initiated by other factors at the neck of endocytic clathrin-coated pits. This was of special interest since prominent dynamin binding proteins that colocalize with dynamin at late stage clathrin-coated pits in fibroblasts, such as endophilin 2 (most similar to Rvs167 in yeast)(Perera et al., 2006) and SNX9 (Yarar et al., 2007;Lundmark and Carlsson, 2009), contain BAR domains.

Presence of BAR Domain Proteins at Sites of Tubulation

BAR domains are lipid bilayer binding modules that can sense and/or generate narrow membrane tubules via their arc-shaped structure (Farsad et al., 2001; Peter et al., 2004; Itoh and De Camilli, 2006). Supporting a role of BAR proteins in the dynamics of the tubules, immunofluorescent staining of endogenously expressed endophilin 2 revealed its very robust and punctate cortical accumulation in DKO relative to control cells (Fig. 3 A–C). This phenotype was rescued by expression of dynamin 2-GFP but not of dynamin 2ΔPRD-GFP (Fig. 3C). Endogenous sorting nexin 9 (SNX9), an endocytic factor that like endophilin contains a BAR and an SH3 domain, was also strongly accumulated at the plasma membrane of DKO cells (Fig. 3H and I). Similar but less robust effects for endophilin 2 localization were also observed in cells where dynamin expression was suppressed by dynamin 1 + 2 siRNA transfection (Fig. S3E).

Further analysis of live cells by spinning disk confocal microscopy indicated that endophilin 2-GFP puncta in DKO cells were localized adjacent to clathrin-positive spots, consistent with their presence on the tubular necks of clathrin-coated pits (Fig. 3D and Movie S2). The tubular nature of these structures was most evident at the light microscopy level in thin cellular protrusions where cell geometry helped to constrain the tubules to grow in parallel to the plane of imaging (Fig. 3D and Movie S2). Clathrin-coated pit assembly preceded the formation of endophilin-positive tubules (Fig. 3E). Interestingly, endophilin 2-GFP-positive tubules dynamically formed, elongated and retracted on a minutes-long timescale (Movies S2–4). This was in contrast to the overall stability of clathrin spots (Fig. 3E and Movie S2) and demonstrated that such tubules did not reflect a dead-end pathway arising from the lack of dynamin. The importance of direct membrane interactions of endophilin via the BAR domain was emphasized by observations that the F10E mutation in helix 0, which was shown to block liposome tubulation in vitro (Farsad et al., 2001;Gallop et al., 2006), also prevented its clustering at sites of tubulation in DKO cells (Fig. 3 F and G).

An accumulation at the plasma membrane in the form of spots or short tubules was a general feature observed for transfected GFP- or RFP-tagged forms of multiple dynamin-binding BAR proteins, including endophilin 1, 2 and 3, SNX9, SNX18 (a close homologue of SNX9) (Lundmark and Carlsson, 2009) and M-amphiphysin 2 (Lee et al., 2002)(Fig. 3, 6 and S5). CD2AP-GFP (related to Sla1 in yeast), a protein that like its close homologue CIN85 is a major endophilin binding protein (Petrelli et al., 2002; Soubeyran et al., 2002; Lynch et al., 2003) expressed by fibroblasts (Fig. S4A) which we have found to be recruited before endophilin at clathrin-coated pits of wild type cells (Fig. 3O), also accumulated at the plasma membrane of DKO cells in a punctate pattern that colocalized with endophilin (Fig. 3 J–N). In no case did we observe accumulation of the BAR domain proteins that we tested at the Golgi complex. Collectively, these observations support a role of BAR domain proteins, most likely an overlapping role of several BAR domain proteins, in the formation and/or dynamics of the endocytic tubular invaginations.

F-actin Accumulation at Tubulated Clathrin-Coated Pits

In view of the reported links between dynamin and actin function we next explored the effects of the lack of dynamin on the actin cytoskeleton. A striking and obvious difference between

DKO and control cells in phalloidin staining for F-actin was an increased abundance of punctate F-actin foci at the plasma membrane (Fig. 4A and B). The Arp2/3 complex was co-enriched at these foci (Fig 4C–E) and this phenotype was rescued by re-expression of dynamin 2 but not of the dynamin 2ΔPRD mutant (Fig. 4F). A similarly, although less clear-cut, an altered staining pattern for Arp2/3 was observed upon siRNA-mediated downregulation of dynamin 1 and 2 expression (Fig. S4B). N-WASP (Las17 in yeast) and cortactin, i.e. two proteins that regulate actin nucleation via Arp2/3, and myosin 1E (most similar to Myo 3/5 in yeast (Geli and Riezman, 1996)), an actin-based motor that binds dynamin (Krendel et al., 2007), were also enriched at such foci (Fig. 6O–R and Fig. S4C and D). Co-expression of GFP fused to μ2-adaptin and of an F-actin reporter comprising the calponin homology domain of utrophin (Utr-CH)(Burkel et al., 2007) fused to mCherry revealed that these actin-rich sites correspond to sites of clathrin-mediated endocytosis (Fig. 4G). Accordingly, endophilin accumulations in DKO cells coincided with the F-actin foci (Fig. 4H–J and Movie S3). Quantification of this co-localization in cells co-expressing endophilin 2-GFP and Utr-Ch-mCherry (Fig. 4H) showed that 87.8+/−4.8% (n= 1294 spots examined from 4 cells) of endophilin 2 spots overlapped with F-actin puncta.

Consistent with these findings, close inspection of electron micrographs demonstrated that the tubules of DKO cells were encased in an electron dense matrix (Fig. 2F), which was reminiscent of the actin-based matrix around tubular invaginations of the plasma membrane at endocytic sites (actin patches) in yeast (Mulholland et al., 1994;Kaksonen et al., 2006;Idrissi et al., 2008).

The accumulation of actin foci in DKO cells is triggered by clathrin.

The robust presence of actin at arrested clathrin coated pits fits with the transient presence of actin and actin regulatory proteins previously reported at, at least, a subset of clathrin coated pits (Merrifield et al., 2002; Merrifield et al., 2005; Yarar et al., 2005; Le Clainche et al., 2007). We have confirmed these findings and found that in control cells 84+/−5% (total of 92 pits from 4 cells) of clathrin-coated pits (μ2-GFP) acquired a burst of F-actin (Utr-CH-mCherry) prior to their disappearance (see for example Fig. 4K). A plausible interpretation of these results is that clathrin coats trigger the formation of actin foci, and that under normal conditions the recruitment of dynamin limits actin polymerization and tubule elongation by mediating fission of the budding vesicle. In agreement with this hypothesis, in cells depleted of clathrin by siRNA knockdown (Figure 5A and B) the punctate plasma membrane accumulation of endophilin, cortactin, actin, and Arp2/3 components no longer occurred (Figure 5 C–F). Thus, clathrin coats play a major role in nucleating the assembly of BAR proteins, actin regulatory factors and actin, which in turn triggers tubule formation.

Clathrin-Coated Pit Tubulation Requires an Intact Actin Cytoskeleton

The functional relationship between Arp2/3-mediated actin nucleation and endophilin 2 enrichment at clathrin-coated pits in DKO cells was tested by siRNA knockdown of the p34 (ARPC2) subunit of this complex. This subunit is encoded by a single gene and makes contacts with multiple subunits within the Arp2/3 complex (Robinson et al., 2001). Thus, it is expected that such a perturbation will affect the activity and stability of the whole complex Western blotting confirmed the successful depletion of p34 (Fig. 6A) and immunostaining of knockdown cells revealed loss of the punctate staining pattern of endogenous endophilin 2, suggesting a functional dependence of the endophilin coated tubules on Arp2/3 function (Fig. 6B and C).

Next, the contribution of F-actin to endocytic tubule dynamics was directly and acutely tested using latrunculin B, a drug that blocks actin polymerization by sequestering G-actin. Latrunculin B induced a rapid (within <90 seconds) disappearance of the prominent cortical

F-actin puncta in DKO cells, as detected by loss of phalloidin staining (Fig. S4F) and dispersion of the Utr-CH F-actin reporter (Movie S3). Ultrastructurally, these changes were accompanied (again within <90 seconds) by the reabsorption into the plasma membrane of the long narrow tubular necks of clathrin coated endocytic pits in DKO cells (Fig. 6F–I). Such pits were converted to omega-shaped clathrin coated invaginations connected to the outer cell profile by only short, wide necks (Fig. 6F–I). Consistent with previous reports (Shupliakov et al., 2002;Yarar et al., 2005), latrunculin treatment of control cells also resulted in a predominance of omega shaped pits (Fig. 6E and I) with short wide necks similar to those of DKO cells under such conditions (control neck diameter=61.9+/−3.9nm, DKO=57.1+/− 2.3nm, n= 42 and 73 control and DKO measurements respectively from 3 independent experiments). Thus, actin polymerization contributes to the formation of a narrow neck at clathrin-coated pits and is critical for the elongation of this neck into a tubule in the absence of dynamin (Fig. 7).

Effects of Actin Depolymerization on the Clustering of Endocytic Factors

Analysis of endocytic proteins following latrunculin B treatment revealed interesting and informative differences among them. As expected, based on EM observations and previous studies (Merrifield et al., 2005; Moskowitz et al., 2005; Yarar et al., 2005), clathrin (GFP-CLC) did not disperse (data not shown). Endophilin 2-GFP, its binding partner CD2AP-GFP (Fig. 6J–N and Movies S3–S7) and myosin 1E (Fig. 6O and Movie S8) dispersed, supporting their selective, F-actin dependent, association with the narrow tubules. The dynamic nature of the actin-dependent recruitment of endophilin is further demonstrated by the rapid re-clustering of endophilin upon washout of latrunculin B (Movie S6). In contrast, GFP-N-WASP, an actin regulatory protein that acts at the plasma membrane upstream of the Arp2/3 complex (Takenawa and Suetsugu, 2007), did not disperse in response to latrunculin (Fig. 6P and Movie S7). However, its fluorescence became even more locally confined to small spots, most likely accompanying the collapse of tubulated pits to omega shaped endocytic pits under these conditions. SNX9, which contains a BAR domain, also lost its tubular localization but residual fluorescence was detectable as discrete spots after actin depolymerization (Fig. 6S and Movie S9). This fraction of SNX9 possibly reflected a pool of the protein localized at the collapsed pits due to the persistence of its known interactions with N-WASP (Yarar et al., 2007), endocytic clathrin coat components and integral membrane proteins (Lundmark and Carlsson, 2009).

This actin-dependence of the BAR domain coated tubules at the base of clathrin coated pits in DKO cells was striking and unexpected as these BAR domain proteins can tubulate the plasma membrane in a latrunculin-insensitive manner in other contexts [see below and (Itoh et al., 2005)]. However, consistent with an actin-dependent role for this module of proteins in the normal progression of clathrin-coated pits, we found that even in control cells that the transient recruitment of endophilin 2 and of CD2AP (an endophilin and F-actin binding protein) was rapidly lost in response to latrunculin (Fig. 6L and M and Movies S4 and S5).

It is important to note that the actin-dependent, clathrin-capped tubules of dynamin DKO cells, which collapse upon latrunculin B treatment, differ from the non-clathrin capped tubules positive for BAR domain proteins that are triggered by latrunculin B treatment (Itoh et al., 2005). Accordingly, following the latrunculin B treatment, new very different (> 1 μm long, generally straight) BAR domain protein-positive tubules started to grow in both control and DKO cells (Movies S4 and S6). This finding emphasizes that an intact actin cytoskeleton is not generally required for BAR domain mediated membrane tubulation but rather is absolutely critical for membrane tubulation in the context of a budding endocytic clathrin-coated pit in a living cell.

DISCUSSION

In this study, by eliminating dynamin expression we have obtained new insight into the molecular network that functions upstream of this GTPase in clathrin-mediated endocytosis. Our results demonstrate a coordinated action of the actin cytoskeleton and BAR domain proteins at clathrin-coated pits, which in the absence of dynamin results in the tubular elongation of their necks. The assembly of this protein network and the formation of the tubules is seeded by clathrin coat assembly, dependent on actin polymerization, propagated by further actin polymerization and BAR protein accumulation, and terminated by dynamin dependent membrane fission under physiological conditions (summarized in Fig. 7). These findings fit with the observation that many of the preferred interacting partners of dynamin are membrane tubulating proteins and/or actin regulatory proteins (Ringstad et al., 1997;Slepnev and De Camilli, 2000;Conner and Schmid, 2003;Orth and McNiven, 2003;Schafer, 2004;Itoh and De Camilli, 2006;Yarar et al., 2007) and show that such proteins act, at least in part, upstream of dynamin at endocytic clathrin-coated pits. While roles of actin nucleating proteins, actin and BAR proteins in clathrin-mediated endocytosis were shown by previous studies, many questions remained open about their specific sites of action and relationships to one another within the molecular steps underlying this endocytic process.

The structures that accumulate in the absence of dynamin in mammalian fibroblasts have a major resemblance to yeast actin patches (Kaksonen et al., 2006)(Fig. 7) and emphasize the evolutionarily conserved action of the factors involved in their formation. At actin patches, short, clathrin-capped tubular invaginations encased in, and supported by, an actin matrix and BAR proteins, represent the endocytic intermediate preceding vesicle fission (Kaksonen et al., 2005; Idrissi et al., 2008). The tubules of DKO cells are generally much longer and are more clearly capped by a vesicular clathrin-coated bud. However, tubules of yeast actin patches have a similar diameter and are surrounded by a similar molecular network (Mulholland et al., 1994; Kaksonen et al., 2005; Idrissi et al., 2008). Furthermore, our results demonstrate that the sequence of recruitment of components of this network is generally the same in yeast (Kaksonen et al., 2006) and mammalian cells (this study). One difference is observed for Sla1, whose recruitment precedes actin accumulation in yeast (Kaksonen et al., 2003; Kaksonen et al., 2005), in contrast to the recruitment after actin of its partial homologue CD2AP/CIN85. However, Sla1 is additionally a cargo adaptor (coat protein), and while CD2AP/CIN85 possess common scaffolding and actin binding domains with Sla1(Lehtonen et al., 2002), they do not contain the domain of Sla1 that is responsible for its cargo adaptor function (Howard et al., 2002). Based on all these findings, we interpret the actin-dependent tubular necks at the base of clathrin-coated pits as being homologous to yeast actin patches. Why yeast cells do not require dynamin for endocytic vesicle fission (Kaksonen et al., 2006) remains a key open question. Perhaps, the presence of a cell wall and/or an increased turgor pressure in yeast affects the biophysical parameters of endocytosis (Aghamohammadzadeh and Ayscough, 2009).

Direct interactions of dynamin with cortactin and other actin regulatory factors suggested an interplay between dynamin and actin but did not clarify whether actin could have a function upstream of dynamin. Likewise, several studies have implicated actin at multiple stages of clathrin-coated pit maturation, including early stages (Shupliakov et al., 2002; Yarar et al., 2005) fission itself (Merrifield et al., 2002; Merrifield et al., 2005) or post-endocytic vesicle movement (Merrifield et al., 2002). Observations of the temporally similar recruitment of endophilin and dynamin to clathrin-coated pits in wildtype cells (Perera et al., 2006) did not elucidate the order of their recruitment. Our new results demonstrate a dynamin-independent contribution of actin polymerization in the constriction and deep invagination of endocytic clathrin-coated pits just prior to dynamin-mediated membrane fission, although they are compatible with additional roles of such proteins and actin during and/or after fission.

Actin polymerization is not an absolute requirement for the membrane tubulating activity of the BAR domain proteins that bind dynamin such as endophilin and amphiphysin. These proteins can tubulate protein-free liposomes (Takei et al., 1999; Farsad et al., 2001; Peter et al., 2004) and even produce long tubular invagination of the plasma membrane of living cells under conditions where the actin cytoskeleton has been disrupted (Itoh et al., 2005)(Movies S4 and S6). Both these conditions favor tubulation due to low membrane tension. However, the tubulating activity of these proteins is specifically harnessed in an actin-dependent manner in the physiologically relevant context of shaping the neck of clathrin-coated pits and this function becomes even more evident in the absence of dynamin. Under these conditions, the curvature sensing properties of BAR domains may predominate over their curvature generating properties and they could help stabilize, and then propagate, a tubular constriction generated by other actin-dependent mechanisms. Additionally, or alternatively, the presence at nascent endocytic sites of proteins that bind F-actin as well as BAR proteins- for example the endophilin-binding proteins CD2AP/CIN85 (Petrelli et al., 2002; Soubeyran et al., 2002; Lynch et al., 2003)- may help, in cooperation with coat components and cargo that recruit BAR proteins (Tang et al., 1999; Slepnev and De Camilli, 2000; Lundmark and Carlsson, 2009), in enriching them to the critical concentration needed for membrane binding and tubulation.

We have observed that lack of dynamin results in a robust accumulation of F-actin at clathrin-coated pits. Conversely, it is expected that conditions that favor rapid dynamin recruitment and function will minimize the opportunity and requirement for actin polymerization at endocytic sites (Fig. 7). The persistence of clathrin-mediated, dynamin-dependent endocytic events after actin disruption (Moskowitz et al., 2005;Yarar et al., 2005;Saffarian et al., 2009) is consistent with this possibility. Under such conditions, dynamin could be recruited by an actin-independent mechanism. The multiplicity of indirect interactions of dynamin with endocytic proteins highlights the variety of pathways that likely contribute to concentrating this GTPase at clathrin-coated pits. For example, recruitment of dynamin could still proceed in the absence of actin via interactions with BAR proteins that bind clathrin, AP-2 or cargo proteins (Tang et al., 1999;Slepnev and De Camilli, 2000;Lundmark and Carlsson, 2009). Such recruitment could be further facilitated by the curved template of the clathrin coated pit neck (Fig. 7, bottom). These considerations could explain the variability of results concerning the role of the actin cytoskeleton in clathrin-mediated endocytosis depending upon the cell types and contexts examined (Shupliakov et al., 2002;Sankaranarayanan et al., 2003;Merrifield et al., 2005;Moskowitz et al., 2005;Yarar et al., 2005;Le Clainche et al., 2007). Clathrin-coated endocytic pits with long tubular necks have been described previously in wildtype fibroblasts (Willingham and Pastan, 1983). The striking resemblance of such tubulated clathrin-coated pits to the ones described here raises the possibility that they originated due to an impairment of dynamin's activity under the specific conditions used for such experiments (Goldenthal et al., 1984). Regulation of dynamin activity may occur in the context of normal cellular physiology to coordinate cargo recruitment with membrane fission.

While our results can be explained by a model whereby dynamin limits elongation of tubular necks of clathrin-coated pits by triggering fission, our observations are also compatible with a direct action of dynamin as a negative regulator of actin polymerization at clathrin-coated pits. We note that functions of dynamin in regulating cytoskeleton dynamics independent from clathrin-mediated endocytosis have been proposed (Henley et al., 1998; Cao et al., 2000; Ochoa et al., 2000; Lee and De Camilli, 2002; Orth et al., 2002; Kaksonen et al., 2005; Liu et al., 2008; Mooren et al., 2009; Tanabe and Takei, 2009). These potential functions of dynamin should be further explored. However, as the block of clathrin-mediated endocytosis and the sequestration at arrested pits of actin regulatory and endocytic factors produced by the lack of dynamin is expected to have effects on signaling, as well as on a variety of other cellular parameters, at least some of the non-endocytic, structural and functional changes that have

been observed in cells with impaired dynamin function may be indirectly connected to the major function of dynamin in endocytosis.

In conclusion, our results provide new information on the sequence of events that underlie clathrin-mediated endocytosis, strengthens evidence a highly conserved function of actin in this process that extends from yeast to mammals, reveal an intimate relationship between the actin cytoskeleton and BAR proteins, demonstrates a sequential connection between the endocytic function of actin and dynamin and show that the functional link between dynamin and actin is closely linked to the endocytic function of this GTPase.

EXPERIMENTAL PROCEDURES

Gene Targeting Strategies

The dynamin 2 conditional KO targeting strategy (Fig. S1) flanked a 1.5kb region containing exon 2 with loxP sites and inserted an FRT site flanked neomycin resistance cassette into intron 2. The dynamin 1 (Dnm1 gene symbol, mouse chromosome 2) conditional KO targeting vector flanked exons 2–4 with loxP sites, inserted an FRT site flanked neomycin resistance selection cassette into intron 1 and contained a 5' thymidine kinase negative selection cassette (Fig. S1). Animal care and use was carried out in accordance with our institutional guidelines. A detailed explanation of gene targeting methods is presented as Supplemental Data.

Fibroblast Cultures

Fibroblasts were isolated from KO and conditional KO mice from the age of embryonic day 12 to post-natal day 1 and grown by standard methods. Delivery of Cre recombinase was achieved by transfection, viral transduction or by 4-hydroxytamoxifen (OHT) activation of a Cre recombinase-estrogen receptor fusion protein encoding transgene. Each method resulted in dynamin depletion and the appearance similar phenotypes over an interval of ~ 5 days. See Supplemental Experimental Procedures for full details.

Antibodies

Immunoblotting of cultured fibroblasts was performed by previously described methods (Ferguson et al., 2007). The sources of the antibodies used in this study are summarized in the Supplemental Experimental Procedures.

siRNA Transfection

Cells were transfected with siRNA (150 pmol/transfection, IDT) using RNAiMAX (5μl/transfection, Invitrogen) and were used for experiments 3–5 days later to allow for target degradation. Sequences of the siRNAs are provided in the Supplemental Experimental Procedures.

Assays for Characterization of DKO Cells

Cell proliferation was quantified by either direct counting or by antibody based detection of BrdU incorporation. Transferrin uptake was measured using Alexa594 conjugated human transferrin (Invitrogen). Transferrin receptor biotinylation was achieved using EZ-link Sulfo-NHS-SS-Biotin with subsequent protein recovery on Neutravidin beads (Thermo Scientific, Rockford, IL). For FM1-43FX uptake, fibroblasts were incubated for 30 minutes at 37°C in 5μg/mL FM1-43FX (fixable analog of FM1-43, Invitrogen), washed, fixed in 4% paraformaldehyde-0.1M sodium phosphate pH 7.2, mounted in Prolong Gold (Invitrogen) and imaged as for the immunofluorescence experiments described below. These methods are described in detail in the Supplemental Experimental Procedures.

Electroporation, Plasmids and Reagents

Cells for imaging experiments were electoporated with the Amaxa Nucleofector method and were plated at sub-confluent densities into 2.5μg/ml human fibronectin (Millipore)-coated 35 mm glass bottom (thickness=1.5) dishes (Mattek, Ashland, MA) and allowed to grow for 12 to 48 hours prior to imaging. Details of plasmid construction and acquisition from other labs are presented in the Supplemental Experimental Procedures.

Immunofluorescence

Cells were grown on either untreated or 5μg/ml fibronectin (Millipore) coated glass coverslips and were fixed with 4% paraformaldehyde-0.1M sodium phosphate pH 7.2, washed with 50mM NH_4Cl pH 7.2, then blocked and permeablized with PBS+3% bovine serum albumin + 0.1% TX100. Subsequent primary and secondary antibody incubations were made in this buffer. Coverslips were finally mounted in Prolong Gold (Invitrogen). For epifluorescence imaging, samples were imaged with a Zeiss Axioplan2 microscope using a Plan-Apochromatic 40× objective and a Hamamatsu (Bridgewater, NJ) ORCA II digital camera under the control of MetaMorph v7.1.2 software (Molecular Devices, Sunnyvale, CA). Alternatively, as indicated, immunofluorescence data was also acquired by spinning disk confocal microscopy (see below).

Widefield Video Microscopy

Imaging was performed at 30–37°C in the following buffer: 136mM NaCl, 2.5mM KCl, 2mM CaCl2, 1.3mM MgCl, 10mM glucose, 10mM HEPES supplemented with 2.5% fetal bovine serum. Time-lapse widefield epi-fluorescent images were acquired with a Leica AM6000 inverted microscope equipped with Plan- Apochromatic 40X oil and 63X glycerol immersion objectives, and a CoolSnap HQ CCD camera (Photometrics, Pleasanton, CA). A 470/30 nm excitation and 520/35 emission filter was used for GFP imaging. Image capture and data acquisition were performed using Metamorph software V7.0r1. Images were acquired at 0.25–0.5 Hz and exposure times of 100–300 ms. Images sequences were subsequently processed with Metamorph and ImageJ software (1.40g, NIH).

Spinning Disk Confocal Microscopy

Spinning disc confocal microscopy was performed using the Improvision (Waltham, MA) UltraVIEW VoX system including a Nikon Ti-E Eclipse inverted microscope (equipped with 60x CFI PlanApo VC, NA 1.4, and 100x CFI PlanApo VC, NA 1.4 objectives) and a spinning disk confocal scan head (CSU-X1, Yokogawa) driven by Volocity (Improvision) software. Images were acquired without binning with a 14 bit (1000×1000) Hamamatsu (Bridgewater, NJ) EMCCD. Illumination was provided by Coherent solid state 488 nm/50 mW diode and Cobolt (Stockholm, Sweden) solid state 561 nm/50 mW diode lasers. Emission filters for GFP and RFP were: a 527 nm band single band pass center wavelength (CWL), 55 nm half-power bandwidth (FWHM) and a double band pass 500–548 nm and 582–700 nm respectively. Typical exposure times and acquisition rates were 100–300 ms and 0.25 Hz respectively. Cells were imaged at temperatures ranging from 23–37°C. Where indicated, images were taken at 100 nm intervals in the Z-axis, iteratively deconvolved with Volocity software and presented as maximal projections. Background signals were reduced by the use of a 3 pixel filter (Volocity). Post-acquisition image analysis was performed with Volocity as well as ImageJ software.

Electron Microscopy

Control and DKO fibroblasts (~80% confluent) in 60mm dishes were fixed in 2% glutaraldehyde-0.1M sodium cacodylate. After gentle scraping and pelleting, subsequent electron microscopy and tomography procedures were performed as previously described

(Ferguson et al., 2007; Hayashi et al., 2008). Details of morphometric analysis are presented in the Supplemental Experimental Procedures section.

Supplementary Material

Refer to Web version on PubMed Central for supplementary material.

Acknowledgments

We thank Frank Wilson, Lijuan Liu, Louise Lucast and Livia Tomasini for superb technical assistance, Dr. Tim Nottoli (Yale Cancer Center Animal Genomics Shared Resource) for help with gene targeting. Many generous gifts of key reagents are acknowledged in the Supplemental Experimental Protocols section. This work was supported in part by the G. Harold and Leila Y. Mathers Charitable Foundation, National Institutes of Health grants to P.D.C. (NS36251, CA46128, DK45735 and DA018343), Grant RR-000592 from the National Center for Research Resources of the National Institutes of Health to J.R. McIntosh, AIRC and Telethon (GGP05141) grants to O.C. and a Canadian Institutes of Health Research fellowship to S.M.F.

REFERENCES

Aghamohammadzadeh S, Ayscough KR. Differential requirements for actin during yeast and mammalian endocytosis. Nat Cell Biol 2009;11:1039–1042. [PubMed: 19597484]

Burkel BM, von Dassow G, Bement WM. Versatile fluorescent probes for actin filaments based on the actin-binding domain of utrophin. Cell Motil Cytoskeleton 2007;64:822–832. [PubMed: 17685442]

Cao H, Thompson HM, Krueger EW, McNiven MA. Disruption of Golgi structure and function in mammalian cells expressing a mutant dynamin. J Cell Sci 2000;113(Pt 11):1993–2002. [PubMed: 10806110]

Conner SD, Schmid SL. Regulated portals of entry into the cell. Nature 2003;422:37–44. [PubMed: 12621426]

Cook T, Mesa K, Urrutia R. Three dynamin-encoding genes are differentially expressed in developing rat brain. J Neurochem 1996;67:927–931. [PubMed: 8752097]

Doherty GJ, McMahon HT. Mechanisms of endocytosis. Annu Rev Biochem 2009;78:857–902. [PubMed: 19317650]

Farsad K, Ringstad N, Takei K, Floyd SR, Rose K, De Camilli P. Generation of high curvature membranes mediated by direct endophilin bilayer interactions. J Cell Biol 2001;155:193–200. [PubMed: 11604418]

Ferguson SM, Brasnjo G, Hayashi M, Wolfel M, Collesi C, Giovedi S, Raimondi A, Gong LW, Ariel P, Paradise S, et al. A selective activity-dependent requirement for dynamin 1 in synaptic vesicle endocytosis. Science 2007;316:570–574. [PubMed: 17463283]

Gallop JL, Jao CC, Kent HM, Butler PJ, Evans PR, Langen R, McMahon HT. Mechanism of endophilin N-BAR domain-mediated membrane curvature. Embo J 2006;25:2898–2910. [PubMed: 16763559]

Geli MI, Riezman H. Role of type I myosins in receptor-mediated endocytosis in yeast. Science 1996;272:533–535. [PubMed: 8614799]

Goldenthal KL, Pastan I, Willingham MC. Initial steps in receptor-mediated endocytosis. The influence of temperature on the shape and distribution of plasma membrane clathrin-coated pits in cultured mammalian cells. Exp Cell Res 1984;152:558–564. [PubMed: 6144562]

Hayashi M, Raimondi A, O'Toole E, Paradise S, Collesi C, Cremona O, Ferguson SM, De Camilli P. Cell- and stimulus-dependent heterogeneity of synaptic vesicle endocytic recycling mechanisms revealed by studies of dynamin 1-null neurons. Proc Natl Acad Sci U S A 2008;105:2175–2180. [PubMed: 18250322]

Henley JR, Krueger EW, Oswald BJ, McNiven MA. Dynamin-mediated internalization of caveolae. J Cell Biol 1998;141:85–99. [PubMed: 9531550]

Herskovits JS, Burgess CC, Obar RA, Vallee RB. Effects of mutant rat dynamin on endocytosis. J Cell Biol 1993;122:565–578. [PubMed: 8335685]

Hinshaw JE. Dynamin and its role in membrane fission. Annu Rev Cell Dev Biol 2000;16:483–519. [PubMed: 11031245]

Howard JP, Hutton JL, Olson JM, Payne GS. Sla1p serves as the targeting signal recognition factor for NPFX(1,2)D-mediated endocytosis. J Cell Biol 2002;157:315–326. [PubMed: 11940605]

Idrissi FZ, Grotsch H, Fernandez-Golbano IM, Presciatto-Baschong C, Riezman H, Geli MI. Distinct acto/myosin-I structures associate with endocytic profiles at the plasma membrane. J Cell Biol 2008;180:1219–1232. [PubMed: 18347067]

Itoh T, De Camilli P. BAR, F-BAR (EFC) and ENTH/ANTH domains in the regulation of membrane-cytosol interfaces and membrane curvature. Biochim Biophys Acta 2006;1761:897–912. [PubMed: 16938488]

Itoh T, Erdmann KS, Roux A, Habermann B, Werner H, De Camilli P. Dynamin and the actin cytoskeleton cooperatively regulate plasma membrane invagination by BAR and F-BAR proteins. Dev Cell 2005;9:791–804. [PubMed: 16326391]

Kaksonen M, Sun Y, Drubin DG. A pathway for association of receptors, adaptors, and actin during endocytic internalization. Cell 2003;115:475–487. [PubMed: 14622601]

Kaksonen M, Toret CP, Drubin DG. A modular design for the clathrin-and actin-mediated endocytosis machinery. Cell 2005;123:305–320. [PubMed: 16239147]

Kaksonen M, Toret CP, Drubin DG. Harnessing actin dynamics for clathrin-mediated endocytosis. Nat Rev Mol Cell Biol 2006;7:404–414. [PubMed: 16723976]

Kirchhausen T. Three ways to make a vesicle. Nat Rev Mol Cell Biol 2000;1:187–198. [PubMed: 11252894]

Krendel M, Osterweil EK, Mooseker MS. Myosin 1E interacts with synaptojanin-1 and dynamin and is involved in endocytosis. FEBS Lett 2007;581:644–650. [PubMed: 17257598]

Le Clainche C, Pauly BS, Zhang CX, Engqvist-Goldstein AE, Cunningham K, Drubin DG. A Hip1R-cortactin complex negatively regulates actin assembly associated with endocytosis. Embo J 2007;26:1199–1210. [PubMed: 17318189]

Lee E, De Camilli P. Dynamin at actin tails. Proc Natl Acad Sci U S A 2002;99:161–166. [PubMed: 11782545]

Lee E, Marcucci M, Daniell L, Pypaert M, Weisz OA, Ochoa GC, Farsad K, Wenk MR, De Camilli P. Amphiphysin 2 (Bin1) and T-tubule biogenesis in muscle. Science 2002;297:1193–1196. [PubMed: 12183633]

Lehtonen S, Zhao F, Lehtonen E. CD2-associated protein directly interacts with the actin cytoskeleton. Am J Physiol Renal Physiol 2002;283:F734–F743. [PubMed: 12217865]

Liu YW, Surka MC, Schroeter T, Lukiyanchuk V, Schmid SL. Isoform and splice-variant specific functions of dynamin-2 revealed by analysis of conditional knock-out cells. Mol Biol Cell 2008;19:5347–5359. [PubMed: 18923138]

Lundmark R, Carlsson SR. SNX9 - a prelude to vesicle release. J Cell Sci 2009;122:5–11. [PubMed: 19092055]

Lynch DK, Winata SC, Lyons RJ, Hughes WE, Lehrbach GM, Wasinger V, Corthals G, Cordwell S, Daly RJ. A Cortactin-CD2-associated protein (CD2AP) complex provides a novel link between epidermal growth factor receptor endocytosis and the actin cytoskeleton. J Biol Chem 2003;278:21805–21813. [PubMed: 12672817]

Macia E, Ehrlich M, Massol R, Boucrot E, Brunner C, Kirchhausen T. Dynasore, a cell-permeable inhibitor of dynamin. Dev Cell 2006;10:839–850. [PubMed: 16740485]

Merrifield CJ, Feldman ME, Wan L, Almers W. Imaging actin and dynamin recruitment during invagination of single clathrin-coated pits. Nat Cell Biol 2002;4:691–698. [PubMed: 12198492]

Merrifield CJ, Perrais D, Zenisek D. Coupling between clathrin-coated-pit invagination, cortactin recruitment, and membrane scission observed in live cells. Cell 2005;121:593–606. [PubMed: 15907472]

Mooren OL, Kotova TI, Moore AJ, Schafer DA. Dynamin2 GTPase and cortactin remodel actin filaments. J Biol Chem. 2009

Moskowitz HS, Yokoyama CT, Ryan TA. Highly cooperative control of endocytosis by clathrin. Mol Biol Cell 2005;16:1769–1776. [PubMed: 15689492]

Mulholland J, Preuss D, Moon A, Wong A, Drubin D, Botstein D. Ultrastructure of the yeast actin cytoskeleton and its association with the plasma membrane. J Cell Biol 1994;125:381–391. [PubMed: 8163554]

Ochoa GC, Slepnev VI, Neff L, Ringstad N, Takei K, Daniell L, Kim W, Cao H, McNiven M, Baron R, De Camilli P. A functional link between dynamin and the actin cytoskeleton at podosomes. J Cell Biol 2000;150:377–389. [PubMed: 10908579]

Orth JD, Krueger EW, Cao H, McNiven MA. The large GTPase dynamin regulates actin comet formation and movement in living cells. Proc Natl Acad Sci U S A 2002;99:167–172. [PubMed: 11782546]

Orth JD, McNiven MA. Dynamin at the actin-membrane interface. Curr Opin Cell Biol 2003;15:31–39. [PubMed: 12517701]

Perera RM, Zoncu R, Lucast L, De Camilli P, Toomre D. Two synaptojanin 1 isoforms are recruited to clathrin-coated pits at different stages. Proc Natl Acad Sci U S A 2006;103:19332–19337. [PubMed: 17158794]

Peter BJ, Kent HM, Mills IG, Vallis Y, Butler PJ, Evans PR, McMahon HT. BAR domains as sensors of membrane curvature: the amphiphysin BAR structure. Science 2004;303:495–499. [PubMed: 14645856]

Petrelli A, Gilestro GF, Lanzardo S, Comoglio PM, Migone N, Giordano S. The endophilin-CIN85-Cbl complex mediates ligand-dependent downregulation of c-Met. Nature 2002;416:187–190. [PubMed: 11894096]

Praefcke GJ, McMahon HT. The dynamin superfamily: universal membrane tubulation and fission molecules? Nat Rev Mol Cell Biol 2004;5:133–147. [PubMed: 15040446]

Pucadyil TJ, Schmid SL. Conserved functions of membrane active GTPases in coated vesicle formation. Science 2009;325:1217–1220. [PubMed: 19729648]

Ringstad N, Nemoto Y, De Camilli P. The SH3p4/Sh3p8/SH3p13 protein family: binding partners for synaptojanin and dynamin via a Grb2-like Src homology 3 domain. Proc Natl Acad Sci U S A 1997;94:8569–8574. [PubMed: 9238017]

Robinson MS. Adaptable adaptors for coated vesicles. Trends Cell Biol 2004;14:167–174. [PubMed: 15066634]

Robinson RC, Turbedsky K, Kaiser DA, Marchand JB, Higgs HN, Choe S, Pollard TD. Crystal structure of Arp2/3 complex. Science 2001;294:1679–1684. [PubMed: 11721045]

Saffarian S, Cocucci E, Kirchhausen T. Distinct dynamics of endocytic clathrin-coated pits and coated plaques. PLoS Biol 2009;7:e1000191. [PubMed: 19809571]

Sankaranarayanan S, Atluri PP, Ryan TA. Actin has a molecular scaffolding, not propulsive, role in presynaptic function. Nat Neurosci 2003;6:127–135. [PubMed: 12536209]

Schafer DA. Regulating actin dynamics at membranes: a focus on dynamin. Traffic 2004;5:463–469. [PubMed: 15180823]

Shupliakov O, Bloom O, Gustafsson JS, Kjaerulff O, Low P, Tomilin N, Pieribone VA, Greengard P, Brodin L. Impaired recycling of synaptic vesicles after acute perturbation of the presynaptic actin cytoskeleton. Proc Natl Acad Sci U S A 2002;99:14476–14481. [PubMed: 12381791]

Slepnev VI, De Camilli P. Accessory factors in clathrin-dependent synaptic vesicle endocytosis. Nat Rev Neurosci 2000;1:161–172. [PubMed: 11257904]

Soubeyran P, Kowanetz K, Szymkiewicz I, Langdon WY, Dikic I. Cbl-CIN85-endophilin complex mediates ligand-induced downregulation of EGF receptors. Nature 2002;416:183–187. [PubMed: 11894095]

Sweitzer SM, Hinshaw JE. Dynamin undergoes a GTP-dependent conformational change causing vesiculation. Cell 1998;93:1021–1029. [PubMed: 9635431]

Takei K, Haucke V, Slepnev V, Farsad K, Salazar M, Chen H, De Camilli P. Generation of coated intermediates of clathrin-mediated endocytosis on protein-free liposomes. Cell 1998;94:131–141. [PubMed: 9674434]

Takei K, McPherson PS, Schmid SL, De Camilli P. Tubular membrane invaginations coated by dynamin rings are induced by GTP-gamma S in nerve terminals. Nature 1995;374:186–190. [PubMed: 7877693]

Takei K, Slepnev VI, Haucke V, De Camilli P. Functional partnership between amphiphysin and dynamin in clathrin-mediated endocytosis. Nat Cell Biol 1999;1:33–39. [PubMed: 10559861]

Takenawa T, Suetsugu S. The WASP-WAVE protein network: connecting the membrane to the cytoskeleton. Nat Rev Mol Cell Biol 2007;8:37–48. [PubMed: 17183359]

Tanabe K, Takei K. Dynamic instability of microtubules requires dynamin 2 and is impaired in a Charcot-Marie-Tooth mutant. J Cell Biol 2009;185:939–948. [PubMed: 19528294]

Tang Y, Hu LA, Miller WE, Ringstad N, Hall RA, Pitcher JA, DeCamilli P, Lefkowitz RJ. Identification of the endophilins (SH3p4/p8/p13) as novel binding partners for the beta1-adrenergic receptor. Proc Natl Acad Sci U S A 1999;96:12559–12564. [PubMed: 10535961]

Traub LM. Tickets to ride: selecting cargo for clathrin-regulated internalization. Nat Rev Mol Cell Biol 2009;10:583–596. [PubMed: 19696796]

van der Bliek AM, Redelmeier TE, Damke H, Tisdale EJ, Meyerowitz EM, Schmid SL. Mutations in human dynamin block an intermediate stage in coated vesicle formation. J Cell Biol 1993;122:553–563. [PubMed: 8101525]

Willingham MC, Pastan I. Formation of receptosomes from plasma membrane coated pits during endocytosis: analysis by serial sections with improved membrane labeling and preservation techniques. Proc Natl Acad Sci U S A 1983;80:5617–5621. [PubMed: 6136969]

Yarar D, Waterman-Storer CM, Schmid SL. A dynamic actin cytoskeleton functions at multiple stages of clathrin-mediated endocytosis. Mol Biol Cell 2005;16:964–975. [PubMed: 15601897]

Yarar D, Waterman-Storer CM, Schmid SL. SNX9 couples actin assembly to phosphoinositide signals and is required for membrane remodeling during endocytosis. Dev Cell 2007;13:43–56. [PubMed: 17609109]

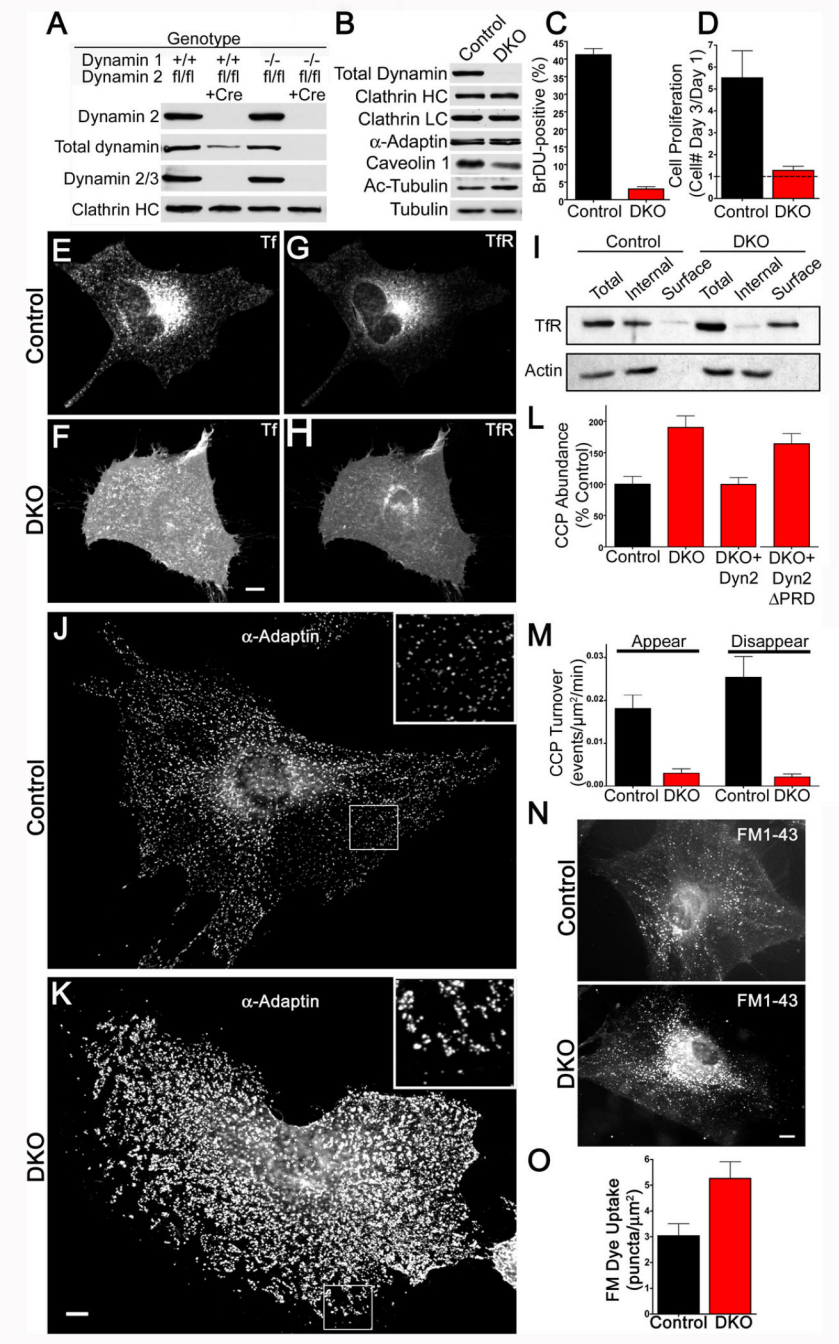

Figure 1.

Cellular proliferation and clathrin mediated endocytosis defects in the absence of dynamin. (A) Immunoblotting analysis with isoform specific antibodies shows that depletion of total dynamin levels from fibroblast cultures requires the KO of both dynamin 1 and dynamin 2. Cells were harvested at 7 days post-transduction with either a control or a Cre recombinase retrovirus. (B) Tamoxifen treatment of $Dnm1^{LoxP/LoxP}$;$Dnm2^{LoxP/LoxP}$;CRE-$ER^{+/0}$ cells depleted total levels of all dynamin proteins, levels of clathrin-coated pit proteins were unaffected, caveolin 1 levels were reduced and levels of acetylated tubulin (Ac-tubulin) were increased. Results are representative of >4 independent experiments. (C) BrDU incorporation in control versus DKO cells (p=0.014, t-test, n=3 experiments). (D) Dynamin DKO cells exhibit

a proliferation defect as revealed by cell counting (p=0.0013, t-test, n=3 experiments). (E) and (F) Uptake of Alexa594 labeled transferrin (Tf) in a representative control cell (E) and DKO cell (F) showing strong intracellular/endosomal versus plasma membrane localizations respectively. (G) and (H) Transferrin receptor(TfR)-pHluorin is predominantly localized in endosomes in control cells (G) and at cell surface in DKO cells (H). (I) Compared to control cells, DKO cells have highly elevated levels of endogenously expressed transferrin receptor in the plasma membrane/biotinylated fraction. (J) and (K) Immunofluorescence (epifluorescence microscopy) staining for the endocytic clatrhin coated pit marker α-adaptin reveals a higher density of pits in the control (J) than in the DKO cell (K). The insets show higher magnifications of the boxed regions. Note that the highly abundant clathrin-coated pits in the DKO cell (K) tend to cluster together. (L) Electroporation with dynamin 2-GFP (Dyn2) but not dynamin 2-ΔPRD-GFP rescued the DKO clathrin-coated pit abundance phenotype. Quantification based on α-adaptin immunostaining (mean+/−SEM, n=12–14 cells/condition). (M) Rates of clathrin-coated pit appearance and disappearance measured from spinning disk confocal imaging of μ2-GFP in Control and DKO cells (n=6 cells/genotype). (N) Representative images of control and DKO cells following uptake of FM1-43 (epifluorescence microscopy). (O) Quantification of FM1-43 uptake (n=10 control and 11 DKO cells respectively). Scale bars represent 10μm. Data are presented as mean+/−SEM. See also Figs. S1 and S2 and Movie S1 for supporting data.

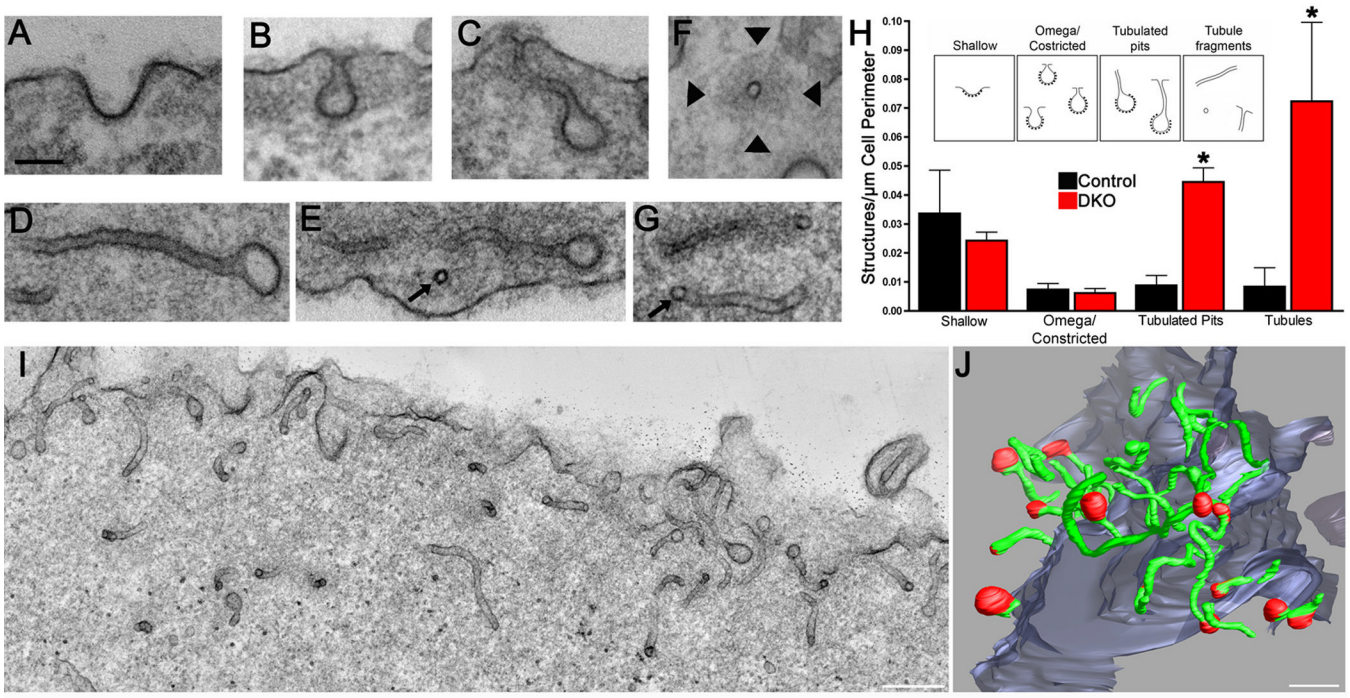

Figure 2.

Massive tubulation of plasma membrane clathrin-coated pits. Representative transmission electron microscopy images of shallow (A), omega-shaped (B) and tubulated clathrin-coated pits (C–E) and tubule fragments (F and G) in DKO cells (~60nm thick sections). Arrows in (E and G) point to cross-sectioned tubules. Arrowheads in F point to the dense cytoskeletal matrix that surrounds a cross-sectioned tubule. The scale bar in panel A=100 nm and applies to panels A–G. (H) Morphometric analysis of electron microscopy images demonstrated the accumulation of tubulated clathrin-coated pits and tubule fragments (t test, p=0.002 and p=0.046 respectively) within 500 nm of the plasma membrane of DKO cells. Inset shows sketches of the structures included in each category. Data was obtained from 3 independent experiments. > 10 cell profiles per genotype were randomly selected for analysis in each experiment. (I) The great abundance of narrow tubules just below the DKO cell surface is evident in this Z-axis maximal projection of 90 slices from a dual axis tomographic reconstruction representing a 180 nm thick sub-volume from the original 250 nm thick section. (J) Electron tomography 3-dimensional reconstruction from single axis tomograms obtained from 3 serial DKO sections (~750 nm total thickness) illustrating the profusion of long, narrow plasma membrane tubules (green) most (13 of 16) of which are capped by clathrin-coated pits (red). Scale bars in (I) and (J) =250 nm. Data are presented as mean+/−SEM.

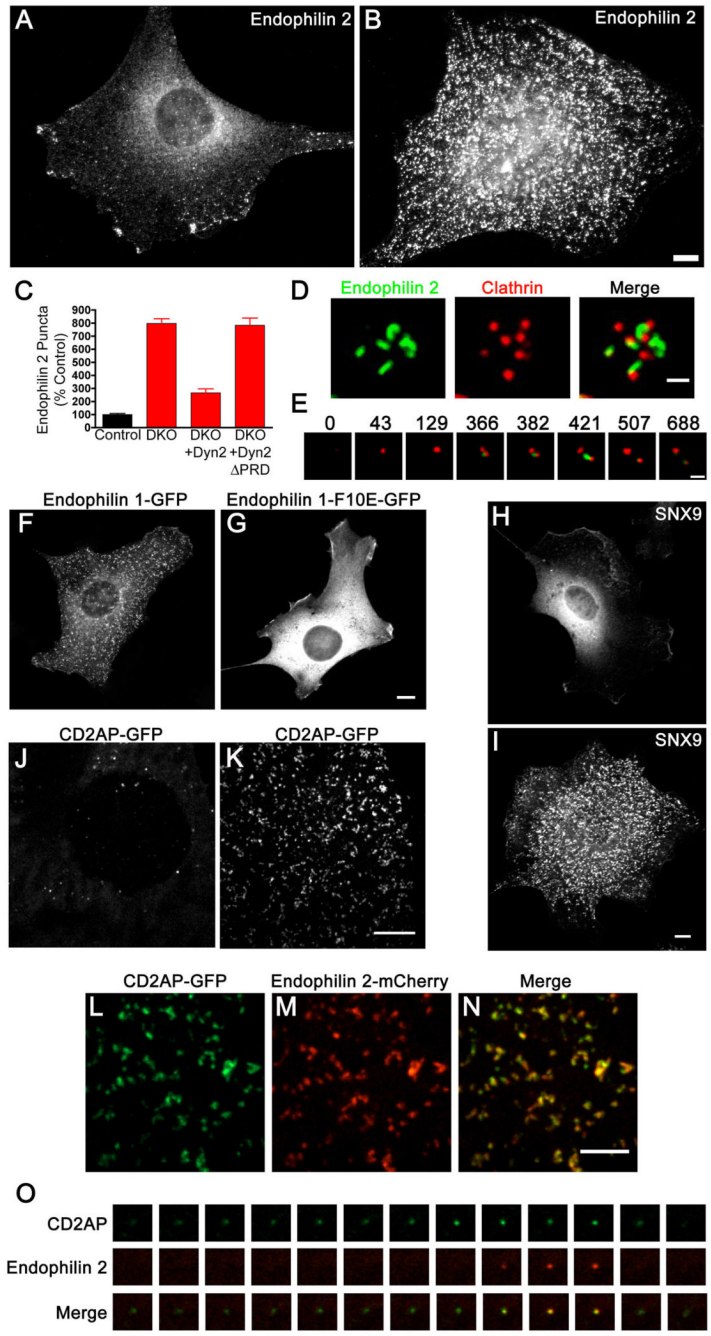

Figure 3.

Dynamin binding BAR domain proteins accumulate at the neck of clathrin-coated pits in DKO cells. (A and B) Endophilin 2 immunoreactivity in control and DKO cells respectively (epifluorescence microscopy). (C) Electroporation with dynamin 2-GFP (Dyn2) but not dynamin 2-ΔPRD-GFP rescued the phenotype of endophilin 2 clustering. Quantification based on immunostaining of endogenous endophilin 2 protein (n=10–21 cells/condition). (D) Spinning disk confocal imaging of endophilin 2-GFP and mRFP-clathrin light chain (LCa) showing the presence of endophilin 2-positive tubules at the base of a cluster of clathrin-coated pits in a DKO cell. (E) Time course showing sequential recruitment of mRFP-LCa (red) and endophilin 2-GFP (green) in a DKO cell. Numbers refer to the relative time in seconds at which

each image was taken. (F) and (G) Endophilin 1-GFP (F) but not the endophilin 1-F10E-mutant (G) exhibits a punctate pattern of localization in DKO cells. (H) and (I) Immunofluorescence staining of endogenous SNX9 in control and DKO cells respectively. (J) and (K) CD2AP-GFP localization pattern in control and DKO cells respectively. (L–N) Co-localization of CD2AP-GFP with endophilin 2-mCherry at the plasma membrane of a DKO cell. (O) Sequence of CD2AP-GFP and endophilin 2-mCherry recruitment to a clathrin-coated pit in a control cell. Frames were taken at 4 second intervals. Panels A, B, F–I are epifluorescence microscopy images, the remainder are spinning disk confocal images. Scale bars for A, B, F–K= 10μm, D and E = 1μm and L–N = 5μm. Data are presented as mean+/−SEM. See also Fig. S3 for and Movies S2 and S5 for supplementary data.

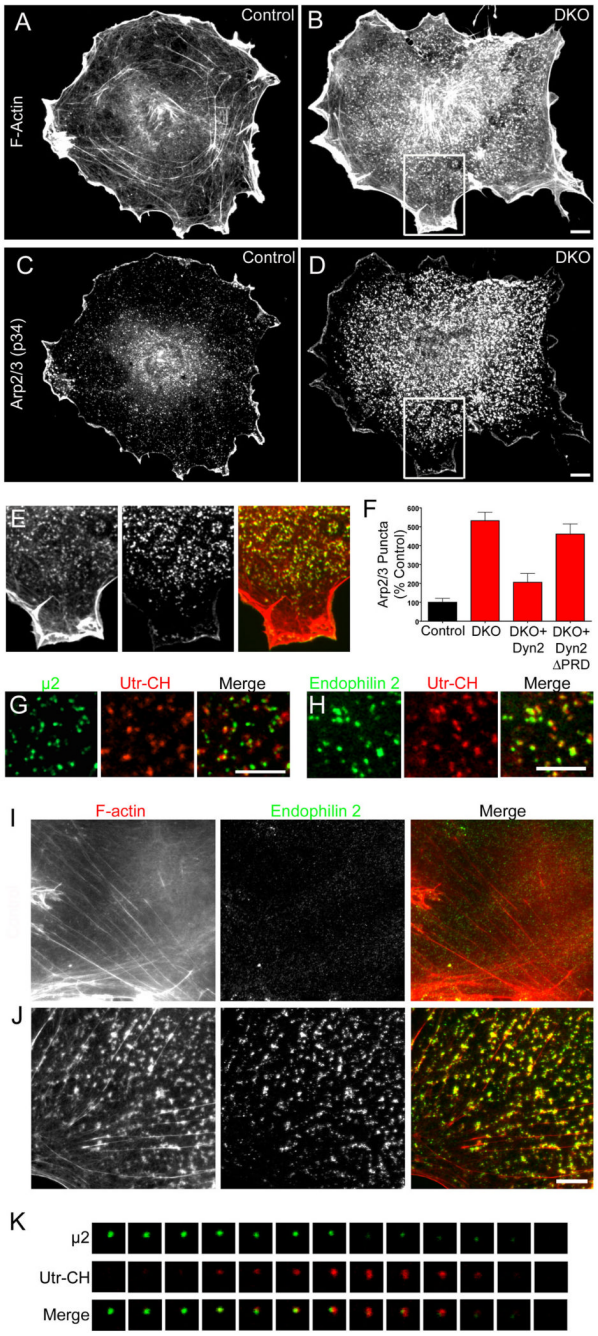

Figure 4.

Enrichment of F-actin at clathrin-coated pits in DKO cells (A and B) Phalloidin staining in control and DKO cells respectively. (C and D) Labeling of the same pair of cells from A and B with anti-Arp2/3 (p34 subunit) antibodies. (E) Merged image of phalloidin (left and red in merged image) and Arp2/3 (middle panel, green in merge) staining from boxed region highlighted in B and D. (F) Quantification of the abundance of Arp2/3 puncta and rescue of the DKO phenotype by dynamin 2 but not dynamin 2ΔPRD (n=9–13 cells/condition). (G) Clathrin-coated pits (μ2-GFP reporter) are sites of F-actin (Utr-CH-mCherry reporter) enrichment in DKO cells. (H) Endophilin 2-GFP and Utr-CH-mCherry co-localize in DKO cells. (I) Control cell double labeled for F-actin (phalloidin staining) and endogenous

endophilin 2 (red=F-actin, green=endophilin 2). (J) Co-localization of F-actin (phalloidin staining) and endogenous endophilin 2 foci in a representative DKO cell (red=F-actin, green=endophilin 2). (K) F-actin (Utr-CH-mCherry) recruitment coincides with clathrin-coated pit (μ2-GFP) disappearance in a control cell. Images taken at 4 second intervals. Scale bars = 10 μm in B, D and H and 5 μm in J. Images in A–E, G and H were acquired by epifluorescence microscopy and by spinning disk confocal in I–K. Data are presented as mean +/−SEM. Supporting data is presented in Figure S4.

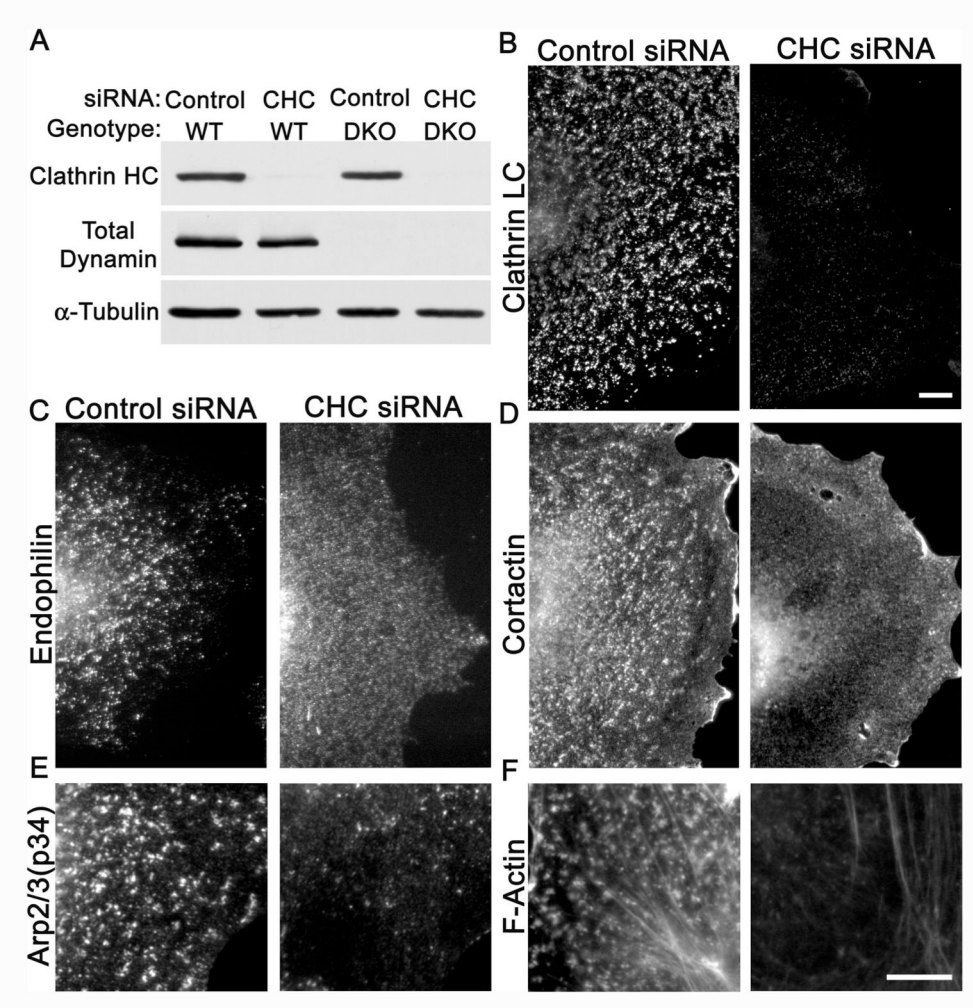

Figure 5.

Clathrin is required for the endophilin and actin phenotypes of DKO cells. (A) Transfection of clathrin heavy chain (CHC) siRNA effectively suppresses clathrin heavy chain protein levels in both wildtype and DKO cells (5 days post-transfection). (B) Suppression of clathrin heavy chain expression depletes clathrin-coated pits from DKO cells as assessed by clathrin light chain immunofluorescence. (C) Endophilin 2, (D) cortactin, (E) Arp2/3 (p34 subunit) and (F) F-actin no longer accumulate in clusters at the plasma membrane of DKO cells lacking CHC. The remaining Arp2/3 puncta are comparable in abundance to those observed in control cells (see Fig. 3E). The 10μm scale bar in panel B applies to B–D. The 10μm scale bar in panel F applies to both E and F. All images were acquired by epifluorescence microscopy.

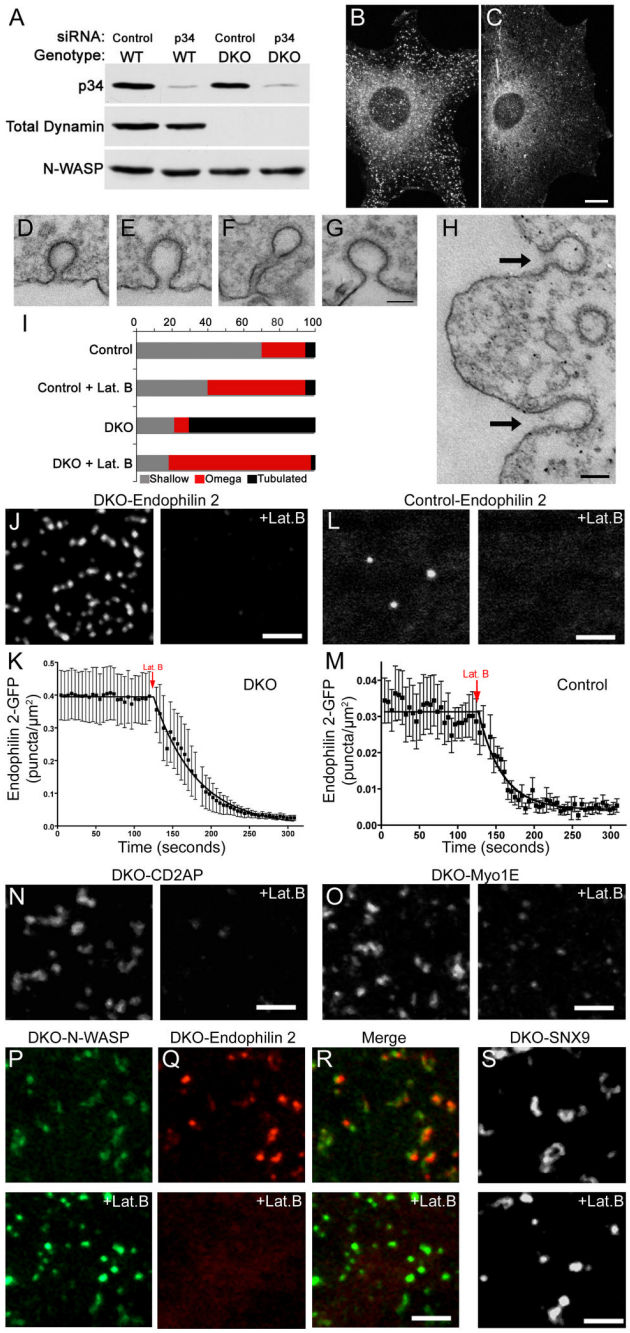

Figure 6.

Tubulation of clathrin-coated pits is acutely dependent on actin polymerization. (A) siRNA-mediated depletion of Arp2/3 complex p34 subunit in control and DKO cells (3 days after transfection). (B) and (C) Representative endophilin 2 immunostaining from control siRNA transfected and Arp2/3 (p34) siRNA transfected DKO cells respectively. (D) Representative example of a clathrin-coated pit from a control cell under basal conditions. (E) Example demonstrating a clathrin-coated pit with a widened neck from a control cell that was fixed after 90 seconds of treatment with 5 μM latrunculin B (Lat. B). (F) A tubulated clathrin-coated pit that is typical of DKO cells under basal conditions. (G and H) Following Lat. B treatment, clathrin-coated pits in DKO cells no longer have long, narrow, tubular necks but are instead

connected to the plasma membrane by short, wide necks. Arrows in (H) point to 2 such pits. (I) Quantification of endocytic clathrin-coated pit morphology in control and DKO cells both before and after latrunculin B treatment. The stacked bars show the percentage of pit structures represented by each morphology under the indicated conditions. Data represents 106 control and 266 DKO clathrin-coated pits randomly identified from 3 independent experiments. (J) Endophilin 2-GFP puncta in DKO cells are dispersed upon Lat. B treatment. (K) Quantification of time lapse imaging of changes in endophilin 2-GFP spot abundance in DKO cells upon Lat. B administration (τ= 56.0 sec, n=8 cells). (L and M) Endophilin 2-GFP recruitment is also Lat. B sensitive in control cells (τ= 30.1 sec, n=11 cells). (N and O) The clustering of CD2AP-GFP and Myo1E-GFP in DKO cells are sensitive to Lat. B. (P–R) GFP-N-WASP (P) becomes brighter and more punctate in DKO cells in response to actin depolymerization with Lat. B while the co-expressed endophilin 2-mCherry (Q) that initially co-localized with N-WASP dispersed. (S) GFP-SNX9 in DKO cells lost its tubular localization and became punctate in response to Lat. B. All representative images of Lat. B treatment (5 μM) correspond a time point 90 seconds after addition of the drug. Scale bars = 10μm in B and C, 100nm in D–H and 2.5 μm in J–S. Images in B and C are maximal projections of deconvolved spinning disk confocal Z-stacks. Images in J–L and N–S are single optical sections from spinning disk confocal microscopy. Data are presented as mean+/−SEM. Data in this figure are further supported by Movies S3–S9.

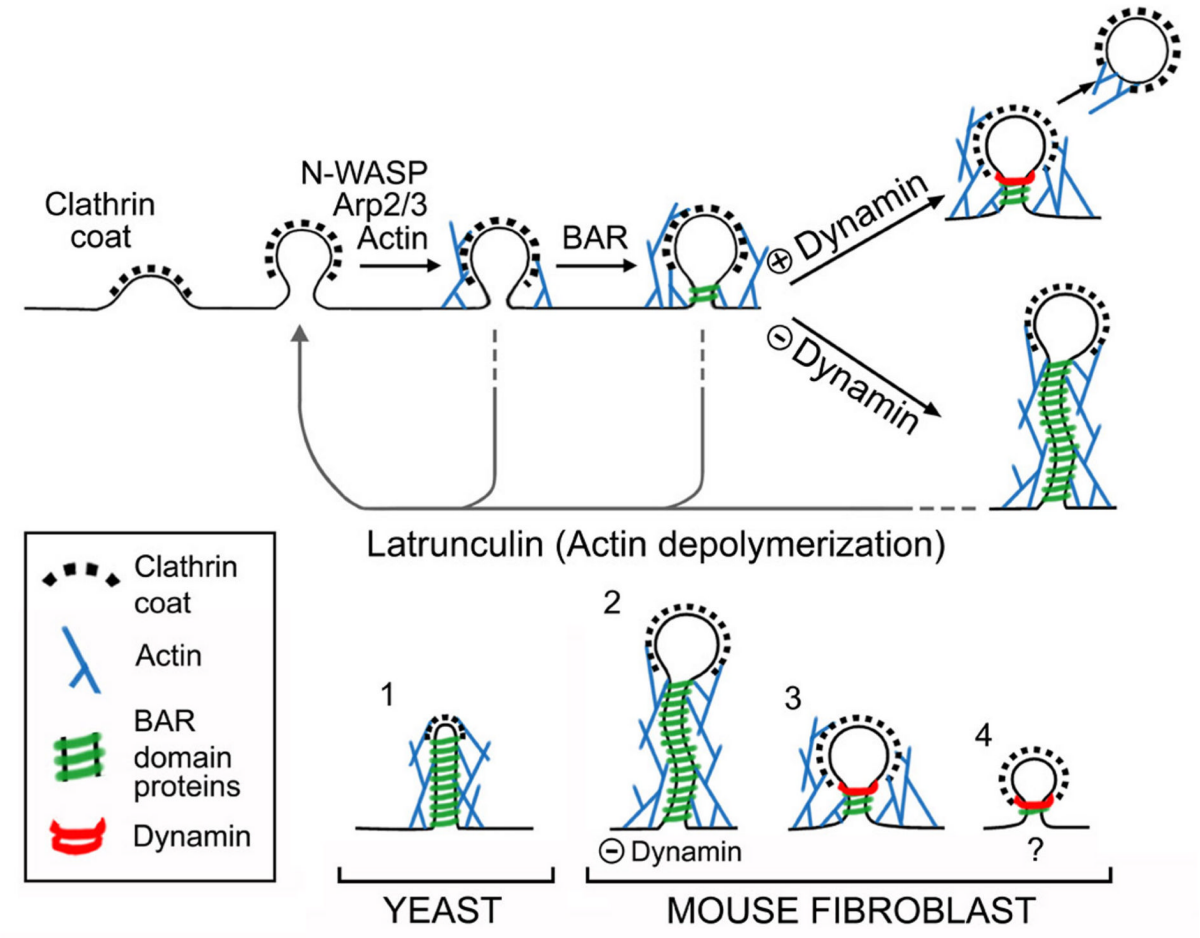

Figure 7.

Diagrams illustrating the sequence of events at mammalian endocytic clathrin coated pits and the evolutionarily conserved relationship between yeast actin patches and clathrin coated pits of higher eukaryotes. Top: Proposed relationship between recruitment of various factors and maturation of endocytic clathrin-coated pits. Dynamin mediates, or contributes to, membrane fission by acting on a tubular template that is generated by growth of the coat and that is further constricted and elongated by a concerted action of actin and BAR proteins. The dynamically extending and contracting tubules observed in the absence of dynamin represent the overgrowth of such templates. Disruption of F-actin by latrunculin leads to collapse of the tubules to a short and wide clathrin-coated pit neck. Bottom: Comparison of clathrin-coated endocytic intermediates and of the molecular machinery supporting their formation in yeast (adapted from Kaksonen et al, 2006) and in mouse fibroblasts. The presence of dynamin in mouse cells (3), but not in yeast (1), minimizes tubule elongation. Lack of dynamin (2) reveals the similarity of events upstream of fission in yeast and fibroblasts. The scenario shown in (4) reflects the reported occurrence of actin-independent clathrin-mediated endocytic events. The membrane curvature sensing properties of BAR proteins and/or the direct or indirect interactions of several BAR proteins with components of the clathrin coat may be sufficient to trigger dynamin recruitment to endocytic pits under such conditions.